Available online at www.sciencedirect.com
SCIENCE DIRECT®
Journal of the European Ceramic Society 25 (2005) 1885–1893
www.elsevier.com/locate/jeurceramsoc

Thermal expansion of $Ca_{1-x}Sr_xZr_4(PO_4)_6$ ceramics

Niloy Chakraborty[a], Debabrata Basu[a], Werner Fischer[b,*]

[a] *Central Glass and Ceramic Research Institute, Calcutta 700032, India*
[b] *Research Center Juelich GmbH, Institute for Processes and Materials in Energy Systems, 52425 Juelich, Germany*

Received 27 March 2004; received in revised form 4 June 2004; accepted 20 June 2004
Available online 26 August 2004

Abstract

Different compounds of the low thermal expansion solid solution series of $Ca_{1-x}Sr_xZr_4(PO_4)_6$ were synthesised by solid-state reaction. Room temperature crystallographic investigations of $CaZr_4(PO_4)_6$ powder samples revealed, that with substitution of Ca by Sr the lattice parameter considerably increased in *c*-direction while the change in *a*-direction was marginally negative. High-temperature X-ray powder diffraction up to 1000 °C pointed out an anisotropic thermal expansion behaviour of these compounds which, however, decreased progressively with increasing Sr content. Sintered samples were prepared from these compounds in which 3 and 5 wt.% ZnO were added to promote sintering. The dilatometric thermal expansion values of the bulk samples are discussed in the light of the corresponding crystallographic data of the powder samples. The results were compared with data published in the literature.

Keywords: Ion-exchange material; Sintering; Thermal expansion; X-ray methods; Functional applications; (Ca, Sr)$Zr_4(PO_4)_6$

1. Introduction

Calcium strontium zirconium phosphate (CSZP), which belongs to the so-called orthophosphate group of $NaZr_2(PO_4)_3$ (NZP) family[1] has emerged as a new class of low-expansion ceramics. The group is characterized by a flexible framework structure belonging to the rhombohedral system with possibility of isomorphic replacements of various groups of elements.[2] In recent years these solid solutions are receiving attention for their potential to be used as (i) ionic conductors[3] and (ii) host material for radioactive waste immobilization because of their structural flexibility with respect to isomorphic ionic replacements and high stability against leaching reactions.[4,5] In addition, these compounds are considered as promising materials for oxidation resistant coating applications on carbon–carbon composites[6] due to their tailorable and low thermal expansion, excellent thermal shock resistance and phase stability at least up to 1000 °C.[5,7–9] The thermal expansion of their crystal lattice is pronounced anisotropic. However, this anisotropy lowers the overall thermal expansion of the bulk material and occasionally results in micro stress induced microcracks during thermal cycles[10] which in turn restricts their more widespread usage.

The attractive thermal expansion properties of these compounds have triggered series of investigations to study the effect of cation substitution on the overall expansion behaviour. Results have been compiled by Taylor[11] and Brewal et al.[12] It has been claimed that with thermal exposure $CaZr_4(PO_4)_6$ (CZP) and $SrZr_4(PO_4)_6$ (SZP) exhibit reverse anisotropy.[13–15] It was reported that with increase in temperature in CZP the *a*-axis contracted and the *c*-axis expanded, while in SZP the opposite behaviour was found. This claim, however, was contradicted by many researchers who observed that the SZP unit cell expanded along both axes with increasing temperature.[5,16] Presently available experimental data on microscopic and bulk thermal expansion of CSZP solid solutions are mostly limited to 600 °C. Therefore, to establish the high-temperature utility of these materials, it is

* Corresponding author.
E-mail address: w.fischer@fz-juelich.de (W. Fischer).

0955-2219/$ – see front matter © 2004 Elsevier Ltd. All rights reserved.
doi:10.1016/j.jeurceramsoc.2004.06.019

felt essential to investigate their phase stability and thermal expansion behaviour at least up to 1000 °C. The tolerance of the unit cell against partial substitution also needs to be studied by crystal structure refinement covering the whole range $0 \leq x \leq 1$ with a step width of 0.25. Results of thermal expansion measurements and the unit cell parameters as a function of temperature and composition of CSZP solid solutions are subject of this paper. Crystal structure data are published in more detail elsewhere.[17]

2. Experimental

2.1. Synthesis and sintering

Five compounds of $Ca_{1-x}Sr_xZr_4(PO_4)_6$ ($x = 0, 0.25, 0.50, 0.75, 1.0$) were synthesized by usual ceramic processing technique through powder mixing followed by solid-state reaction.[13,18,19] The compositions are hereafter referred as CZP, CSZP(I), CSZP(II), CSZP(III), and SZP, respectively. Stoichiometric mixtures of analytical reagent grade powders of $CaCO_3$, $SrCO_3$, ZrO_2, and $NH_4H_2PO_4$ (supplied by M/s S. D. Fine Chemicals, Kolkata, India) were milled in acetone for 6 h in a zirconia lined planetary mill. After air-drying the powder mixture was sieved through 50 US sieve (−297 μm). The processing involved several cycles of heat treatment and subsequent homogenization of the obtained mass in the planetary mill. In the first step the powder mixtures were fused in a muffle furnace at 200 °C/15 h/air to remove water and subsequently calcined at 600 °C/4 h/air to drive-off NH_3 and other volatile components. In the next step the samples were fired once again at 900 °C/16 h/air for decomposition of the carbonates and formation of reactive oxides. Finally, the resultant mass was further calcined at 1300 °C/6 h/air to achieve single phase materials for X-ray powder diffraction measurements.

For the study of sintering a few batch compositions were prepared in which 3 and 5 wt.% ZnO powder was added as sintering aid. Pellet (12 mm in diameter × 10 mm thick) and bar (5 mm × 5 mm × 60 mm) shaped test specimens were prepared by pressing at 50 MPa and subsequent sintering at 1100, 1200 and 1300 °C for 2, 4 and 6 h. The bulk densities of the sintered samples were measured by the usual Archimedean method using distilled water as the displacement liquid.

2.2. Microstructure and composition

Scanning Electron Microscopy was employed for microstructural imaging of the powders (LEO1530, Gemini) and polished surfaces of sintered samples (LEO430i). Energy-dispersive microanalysis (EDX) of the powder samples was carried out using an Oxford Instruments INCA Energy300 system equipped with a HPGe detector. An accelerating voltage of 8 kV was used to ensure the smallest possible interaction volume of the primary electrons within the grains. Though the energy resolution capability of the used HPGe detector with 112 eV at Mn Kα is better than that of a Si(Li) detector, it is still not adequate to resolve the spectral emission lines of the Zr–L and P–K series particularly for a reliable standard-less quantitative analysis. Therefore, and further due to surface roughness of the powders (even selecting a single grain) chemical analysis has been limited to the determination of the Ca/Sr ratios only.

2.3. Dilatometry

Bulk thermal expansion coefficients (TEC) of sintered cylindrical samples were determined from dilatometric measurements using a vertical Shimadzu Thermo-mechanical Analyzer TMA-30 attached with a control unit DT-30. The samples (diameter 4–6 mm, length 12–14 mm) were mounted into an alumina porcelain cell, a load of 5 g was applied, and the elongation during thermal cycles was registered with a Linear Voltage Differential Transformer (LVDT). The LVDT was housed within a closed insulating cover with warm water circulating inside to maintain a constant temperature to avoid any effect of temperature variation on its performance. Bulk TEC was measured in the range 25–1000 °C at a ramp rate of 5 K/min. For each compound, altogether three samples were tested twice and the average value has been reported. The dilatometer calibrated with quartz and copper cylindrical standards (SRM 736) had a sensitivity of $0.1 \times 10^{-6}\,K^{-1}$ for the TEC measurements. A PC based data acquisition system was employed to record thermal expansion data at intervals of 120 s averaged over 10 s at each point.

2.4. X-ray powder diffraction measurements

Prior to high-temperature XRD measurements the powder samples were characterised for their phase purity. Scans have been recorded in the Bragg angle window of 10–100° (2θ) at a Philips (now: Panalytical) X'Pert MRD diffractometer in Bragg-Brentano geometry with Cu Kα radiation.

High-temperature measurements were performed at a Siemens D5000 instrument, equipped with a Buehler HDK S1 high-temperature chamber driven at air. Powder samples were sedimented from an ethanol slurry onto a DC heated Pt strip as approximately 20 μm thick layers. For compensation of elongation during heating, the strip was kept under a slight stress to stabilize the sample height position. The sample temperature was controlled by a Pt/Pt-Rh thermocouple spot-welded to the Pt strip in the middle of the rare side. The maximum temperature error across the illuminated sample area ($20 \times 12\,mm^2$) was estimated by infrared imaging to be within 20 K. Scanning was performed for the Bragg angle window 10–57° (2θ) with 0.02° step width for temperatures 50–1050 °C in intervals of 50 K during the heating-up and the cooling down. The scanning was restricted upto a Bragg angle of 57° to get an acceptable measuring time. Reflections above 57° make only a small contribution to the overall scattered intensity. High(er) angle reflections improve accuracy, of course, but have little influence on the calculation of the

microscopic TEC. Here one should keep in mind the phase purity of the samples discussed later. For temperature stabilisation at every interval the samples were kept for 3 min prior to starting data collection.

2.5. Data evaluation

Structural data were extracted from XRD measurements using the Rietveld refinement method. As starting structural model the hexagonal unit cell of $Cd_{0.5}Zr_2(PO_4)_3$[20] (Inorganic Crystal Structure Database, collection code No. 66820) was used. This unit cell was modified with respect to cell parameters, scattering ions and site occupation. A starting structural model for each compound of the solid solution series was calculated by applying the Rietveld method (Philips X'Pert Plus software) to room temperature data of a corresponding scan from 10 to 100° (2θ).

High-temperature scans were also evaluated by subsequent Rietveld analysis at each temperature. This evaluation strategy had to be applied to take into account remaining fluctuations of the sample height position due to elongation/contraction of the Pt heating strip. Addition of a reference material to the sample powder was not used to avoid reactions with the sample material at elevated temperature. Moreover, since the patterns of CSZP compounds are rich of reflections, it was apprehended that peaks of a reference material would have complicated the data evaluation even further.

Error bars marked in plots represent the sum of estimated accidental errors and uncertainties of Rietveld results caused by the counting statistics and/or curve fitting. Accidental errors were estimated from the scatter of results determined from heating-up and cooling-down and via error propagation.

3. Results

3.1. Microstructure and composition

Fig. 1 shows micrographs of powders of CZP (Fig. 1a and b) and SZP (Fig. 1c and d), respectively. Fig. 1a and 1(c) are secondary electron (SE) images representing mainly topography, while Fig. 1b and d are collected with the backscattered electron (BSE) signal in compositional mode, where mean atomic number information of particles is the contrast dominating feature. The micrographs reveal that although most of the particles are smaller than 1 μm, few larger agglomerates are also present. In both the BSE images few 'darker' particles are visible which are indicative of the presence of a minor secondary phase in the powder. This phase is identified as ZrP_2O_7 (PDF 49-1079), with a mean atomic number

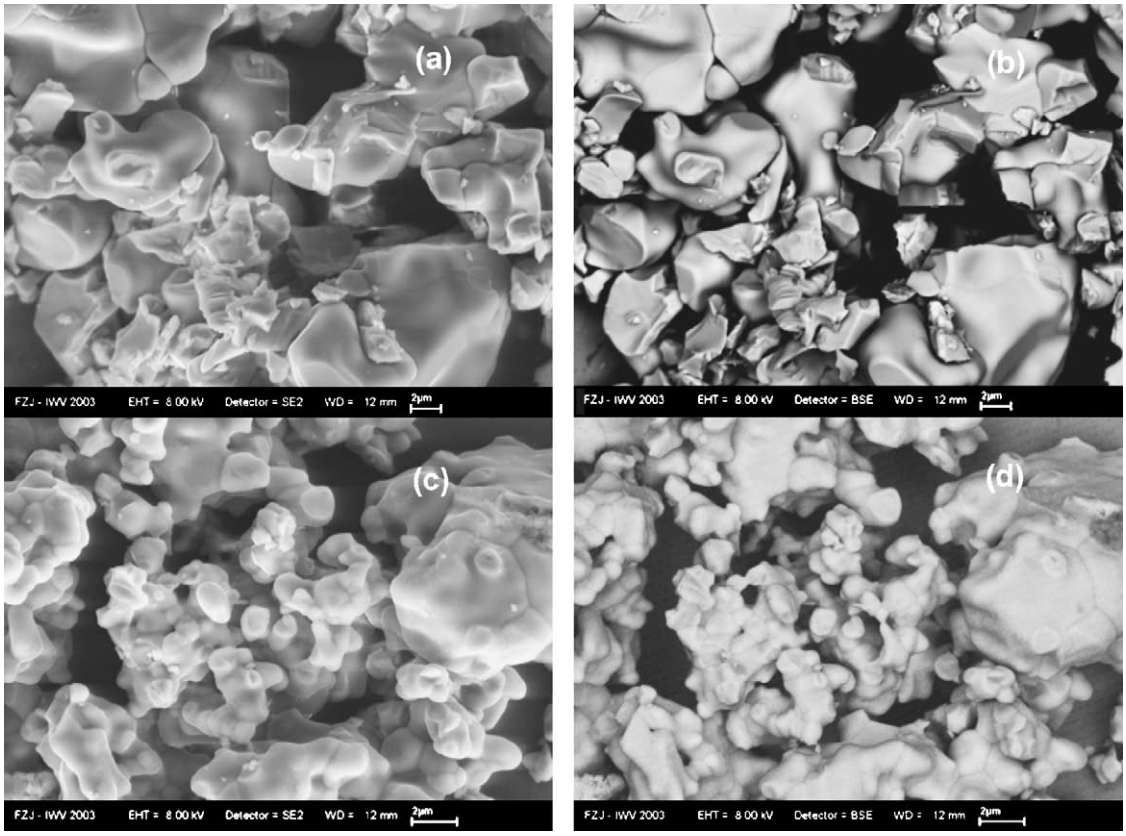

Fig. 1. Morphology of CZP (a and b) and SZP (c and d) powders.

Table 1
Ca/Sr atomic ratio in $Ca_{1-x}Sr_xZr_4(PO_4)_6$ compounds

Sample	Nominal atomic ratio	Experimental atomic ratio
CSZP(I)	3	3.0(2)
CSZP(II)	1	1.0(2)

Table 2
Bulk density of the compounds sintered at 1300 °C for 6 h without sintering aid

Sample	Bulk density (g/cm^3)	Theoretical density (TD) (g/cm^3)	Percentage of TD
CZP	2.53	3.20	79.4
CSZP(I)	2.71	3.23	83.8
CSZP(II)	2.65	3.26	81.2
SZP	2.64	3.33	76.2

Table 3
Bulk linear thermal expansion coefficients of $Ca_{1-x}Sr_xZr_4(PO_4)_6$ compounds in the temperature range 25 °C ≤ T ≤ 1000 °C

Sample	Sintering temperature (°C)	α (10^{-6} K^{-1})
CZP	1300	−2.76(7)
CSZP(I)	1300	0.17(9)
CSZP(II)	1300	0.47(7)
SZP	1300	2.30(5)
CZP + 3 wt.% ZnO	1200	−0.47(10)
CSZP(I) + 3 wt.% ZnO	1200	0.47(11)
CSZP(II) + 3 wt.% ZnO	1200	1.55(7)
SZP + 3 wt.% ZnO	1200	4.00(7)
CZP + 5 wt.% ZnO	1100	0.14(9)
CSZP(I) + 5 wt.% ZnO	1100	0.94(7)
CSZP(II) + 5 wt.% ZnO	1100	1.85(6)
SZP + 5 wt.% ZnO	1100	4.49(9)

smaller than that of either CZP (13.2) or SZP (13.7). The content of ZrP_2O_7 in CZP and CSZP(II) was determined from Rietveld refinement to 7 and 10 wt.%, respectively.

EDX analysis was conducted on flat surfaces of large agglomerates to fulfil the presumption of the matrix correction procedure during quantification of the spectra. Experimental Ca:Sr ratios determined for the samples CSZP(I) and CSZP(II) are given in Table 1. For sample CSZP(III) it was found that the Ca substitution by Sr clearly deviated from the nominal value. Because of this discrepancy between the nominal and the actual composition data of this sample were excluded from evaluations concerning the whole compositional range $0 \leq x \leq 1$.

The bulk density of the CSZP samples fired at 1300 °C for 6 h are compared with the corresponding theoretical densities in Table 2. The maximum bulk density was achieved for CSZP(I), which was only about 84% of the theoretical value. This indicate that to utilize the compounds to their maximum potential in different engineering applications, further work is necessary to increase sinterability of the powders. The effect of ZnO addition on the sintering behaviour of the materials at different heating schedules is summarized in Fig. 2. The compounds with 3 and 5 wt.% ZnO attained bulk densities well over 95% of the corresponding theoretical values when sintered for 2 h at 1200 and 1100 °C, respectively.

Fig. 3 shows the microstructure of sintered CSZP(II) samples with 3 wt.% (Fig. 3a and b) and 5 wt.% (Fig. 3c and d) ZnO added to the compound. Horizontally (Fig. 3a–d) the images reflect the influence of increasing sintering temperature on grain size and porosity. It is evident that irrespective of ZnO content in a compound the average grain size increases when the sintering temperature increases to 1300 °C from 1200 °C for the compound with 3 wt.% ZnO (Fig. 3a and b) and from 1100 °C for the ones with 5 wt.% ZnO (Fig. 3c and d). The microstructure of all the samples shows pores and an irregular micro-crack network which may compensate volume changes during thermal cycling.

3.2. Dilatometric measurements

Dilatometric graphs are shown in Fig. 4. A summary of linear thermal expansion coefficients of bulk samples with and without ZnO additions in the compounds is compiled in Table 3. The TEC of CZP is negative, but it becomes positive already with 25% substitution of Ca ions. This positive TEC increases further with increasing Sr content in a compound.

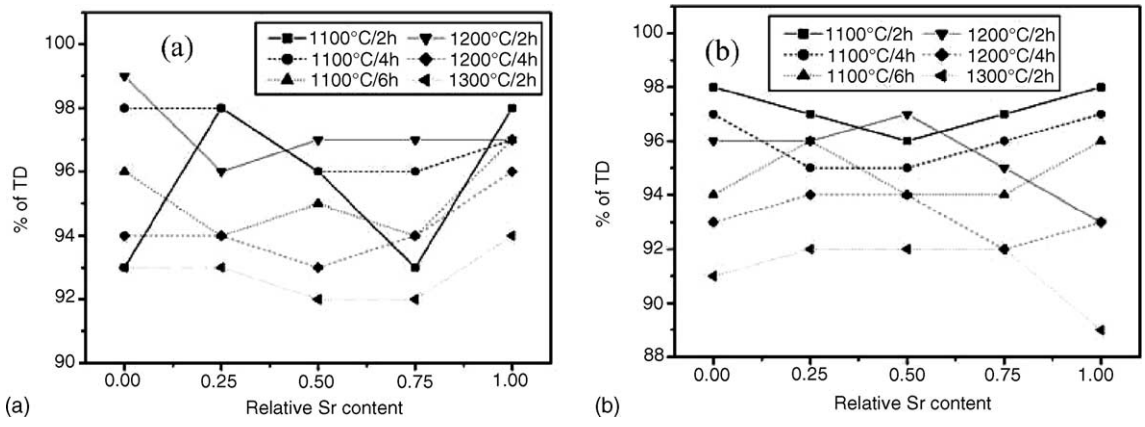

Fig. 2. Sinterability of CSZP compounds with (a) 3 wt.% and (b) 5 wt.% ZnO additions under different firing schedules (temperature/soaking time).

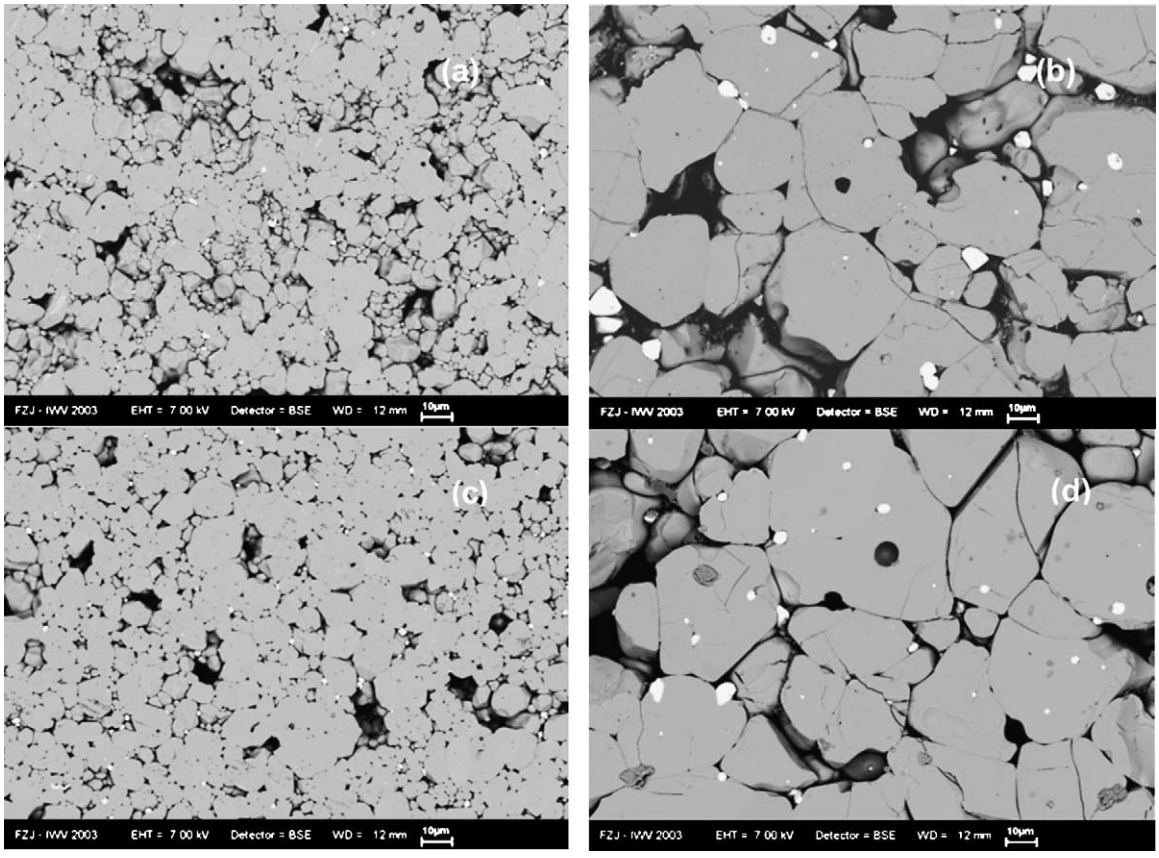

Fig. 3. Scanning electron micrographs of CSZP(II) sintered for 2 h with 3 wt.% ZnO at (a) 1200 °C, (b) 1300 °C and with 5 wt.% ZnO at (c) 1100 °C, (d) 1300 °C.

The addition of a sintering aid, like ZnO in the present study, brings a further significant increase of the TEC values.

3.3. XRD measurements

A comparison of typical phase scans of CZP, CSZP(II), and SZP powders is shown in Fig. 5. These scans indicate that the samples CZP and CSZP(II) contain a small amount of a second phase (ZrP_2O_7, ICDD 49-1073). The most intense free standing reflections of this second phase are labelled (♦). Reflections of the impurity phase were eliminated during Rietveld refinement by setting appropriate 'excluded regions'. The dependence of the hexagonal unit cell parameters on composition is displayed in Fig. 6a.

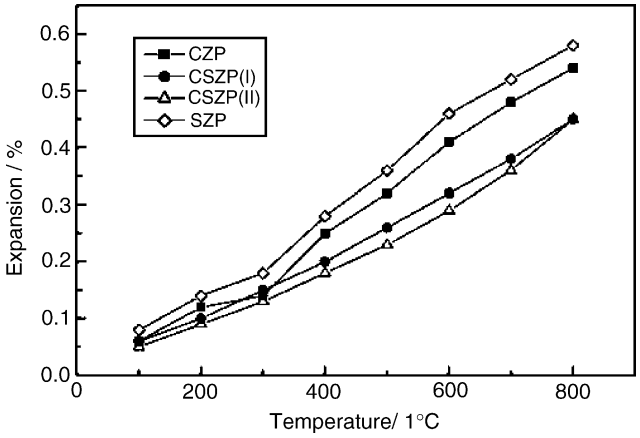

Fig. 4. Dilatometric graphs of CSZP bar shaped samples.

Fig. 6b shows that the ratio c/a as well as the unit cell volume increase linearly with increasing Sr content in the solid solution series. The ratio c/a was found to be 2.58 for CZP which steadily increased with Sr content in the compounds up to 2.68 for SZP while the corresponding unit cell volume also increased from 1511 $Å^3$ to 1525 $Å^3$.

The lattice parameters a and c in dependence of temperature from 25 to 1000 °C are given in Fig. 7. Within the experimental uncertainty both parameters change linearly with temperature. While the slope of a versus T undergoes a reversal with increasing Sr content, the slope of c versus T remains positive for all compounds and becomes steeper from CZP to SZP. Microscopic linear TEC of the samples were calculated by linear regression (Table 4).

Fig. 8 outlines the influence of temperature on the ratio c/a and unit cell volume of these solid solutions. Fig. 8a shows that the slope of c/a versus T decreases progressively with increasing Sr content. For SZP this ratio remains nearly

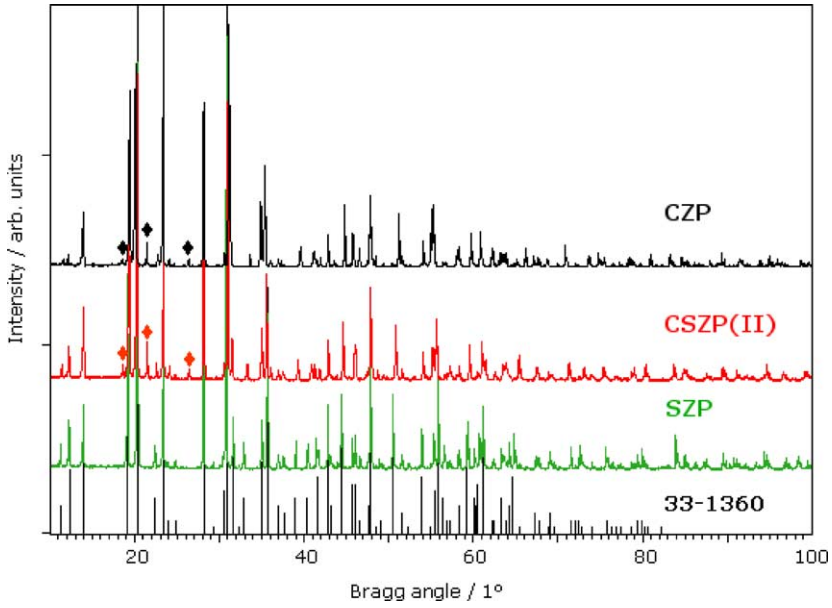

Fig. 5. Powder diffraction patterns of CZP, CSZP(II), and SZP referenced to PDF 33-1360.

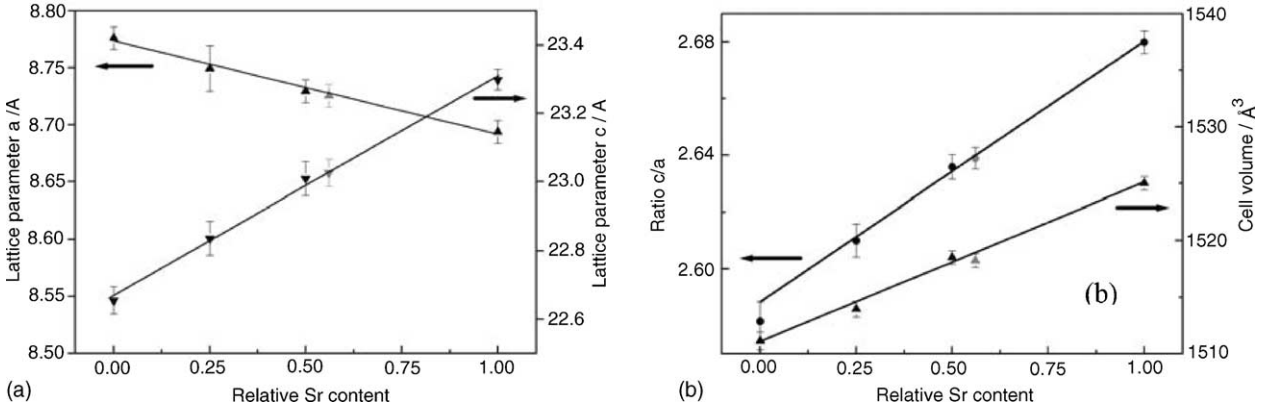

Fig. 6. Lattice parameters (a) and ratio *c*/*a* (b) vs. relative Sr content in CZP solid solutions.

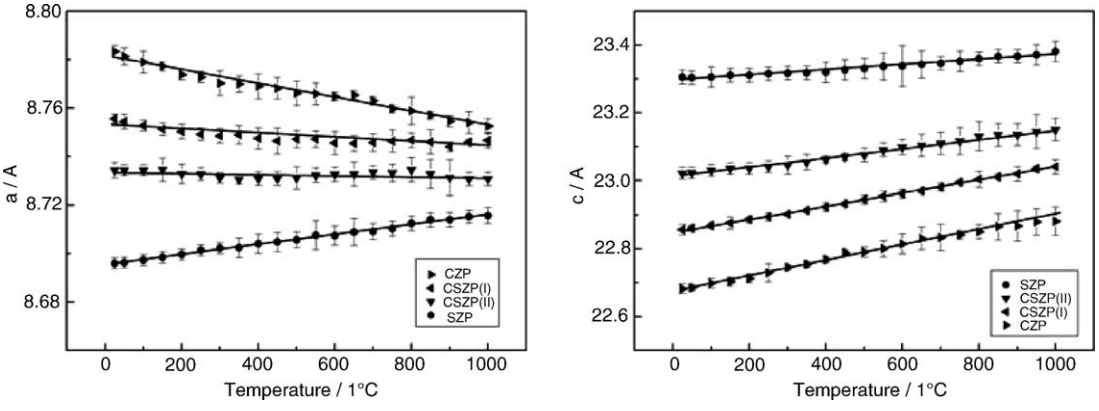

Fig. 7. Lattice parameters *a* and *c* vs. temperature.

Table 4
Lattice parameters of $Ca_{1-x}Sr_xZr_4(PO_4)_6$ at room temperature and microscopic linear TEC in the range 25 °C ≤ T ≤ 1000 °C

Sample	a @ 25 °C/Å[a]	c @ 25 °C/Å[a]	$\alpha_a/10^{-6}\,K^{-1}$	$\alpha_c/10^{-6}\,K^{-1}$
CZP	8.7761(1)	22.6553(4)	−3.3(1)	10.1(2)
CSZP(I)	8.7494(1)	22.8363(5)	−1.0(8)	8.4(1)
CSZP(II)	8.7295(1)	23.0098(5)	−0.2(1)	5.8(2)
SZP	8.6937(1)	23.2988(3)	+0.2(1)	3.3(1)

[a] Calculated from scans at room temperature with 10° ≤ 2θ ≤ 100°.

Table 5
Comparison of bulk thermal expansion coefficients with literature data ($\alpha/10^{-6}\,K^{-1}$).

Sample	This study	Limaye et al.[13] (up to 500 °C)	Angadi et al.[19] (up to 800 °C)
CZP	−2.76(7)	−2.11	−0.9(1)
CSZP(I)	0.17(9)	0.60	0.8(1)
CSZP(II)	0.47(7)	1.40	2.1(1)
SZP	2.30(5)	3.20	2.6(1)

constant over the whole temperature range. The unit cell volume versus temperature (Fig. 8b) shows an increasing slope with increasing Sr content. The thermal expansion of unit cell volume was found to be smallest in CZP.

4. Discussion

The low bulk density of the sintered samples (Table 2) points out that the sinterability of the powders synthesized by solid-state reaction route was poor due to the presence of relatively coarse agglomerates (Fig. 1). Similar observations have been reported by Limaye et. al.[13] who ultimately adapted sol–gel synthesis route to improve sinterability of the powders. In the present case ZnO was added. It significantly densified sintered bodies with a simultaneous reduction of porosity which otherwise would have influenced the bulk properties of the material. By sintering for 2 h at 1200 °C samples with 3 wt.% ZnO could be densified up to 98% of the theoretical density while for the samples with 5 wt.% ZnO the required temperature for getting the same densification was only 1100 °C (Fig. 2). ZnO addition promoted sintering at lower temperature since it reacted with the phosphates under formation of low melting $Zn_3(PO_4)_2$. This reaction generated free ZrO_2 which was evident in the microstructure as white precipitate (Fig. 3). Increase in size of the grains and trapped pores inside the grains were observed in the specimens sintered at higher temperature which in turn reduced their density.

Table 3 shows that for all compounds the bulk thermal expansion coefficients were very low and for pure CZP it was even negative. The values, however, became positive with Sr addition and increased progressively with increasing Sr content. This observation is in agreement with the findings reported in the literature[13,18] and the minor differences in the values (see Table 5) are attributed to the differences in densification and grain size of the corresponding samples. Due to formation of the high expansion $Zn_3(PO_4)_2$ phase during sintering all the compounds with ZnO addition exhibited higher TEC values and obviously this effect was more pronounced in the samples with higher ZnO content. However, even with addition of a sintering aid, the thermal expansion coefficient remained below $4.5 \times 10^{-6}\,K^{-1}$, which establishes the potential of these materials for engineering applications involving thermal cycling.

The low microscopic thermal expansion (Table 4) of this type of compounds can be understood by looking to the crystal structure. The lattice consists of a strongly bonded but flexible three-dimensional network of PO_4 tetrahedra and ZrO_6 octahedra which are interconnected through corner sharing to form a stable hexagonal lattice with structural holes. These holes are occupied by Ca or Sr depending on the composition. Lenain et al.[21] developed a structural model to explain anisotropic and low thermal expansion of these materials. This model operates on rotations of groups within this polyhedral network and coupling between octahedral and tetrahedral groups.

Comparing TEC data of the sintered samples (Table 3) with those obtained by high-temperature XRD

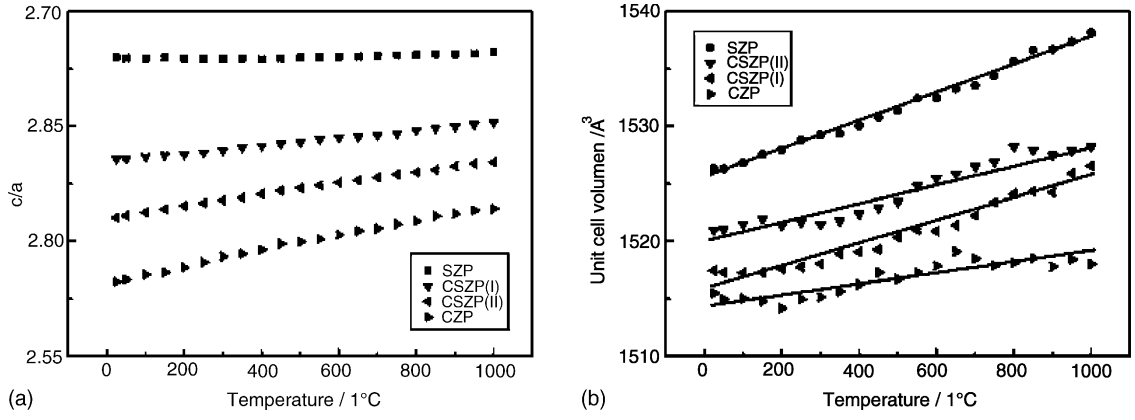

Fig. 8. Ratio c/a (a) and unit cell volume (b) vs. temperature.

Table 6
Comparison of the lattice parameters with literature data

Sample	Lattice parameter, a (Å)			Lattice parameter, c (Å)		
	This study	Angadi et al.[19]	Kutty et al.[22]	This study	Angadi et al.[19]	Kutty et al.[22]
CZP	8.7761(1)	8.785(5)	8.777	22.6553(4)	22.693(14)	22.66
CSZP(I)	8.7494(1)	8.758(5)	–	22.8363(5)	22.920(14)	–
CSZP(II)	8.7295(1)	8.729(4)	–	23.0098(5)	23.119(13)	–
SZP	8.6937(1)	8.701(5)	8.690	23.2988(3)	23.390(13)	23.33

of corresponding powder samples (Table 4) the difference between the two data sets becomes obvious. We believe this difference is caused due to the constraints in the bulk. In a powder sample, the individual crystals are free to expand in any direction without any constraint, while in a bulk the individual grain is bonded to the surrounding ones. This constraint can lead to different TEC for the bulk material.

Table 6 gives a comparison of lattice parameters of this study with those already published in literature.[19,22] The data agree in their general tendency, i.e. there is an elongation in c-direction and a contraction in a-direction with increasing Sr content (Fig. 7a). Since the relative elongation along c-axis (2.8%) is much larger than the contraction in a-axis (−0.9%) the unit cell volume expands with increasing Sr content (Fig. 7b). Assuming a rigid body model, it is clear that the substitution of an ion by a larger one should result in an elongation of the unit cell, however, it is surprising that simultaneously a contraction in the perpendicular a-direction takes place. Lenain et al.[21] and others[23] predicted that due to symmetry restrictions, the PO_4 tetrahedron in this structure is constrained to rotate about a two-fold axis and the ZrO_6 octahedron about a three-fold axis. Since a common oxygen is shared by both the polyhedra, their respective rotation is coupled and therefore to accommodate these constraints simultaneously the atoms undergo a translatory shift changing the lattice parameters. Fig. 9 shows the position of Ca or Sr in a cut-out from the CSZP hexagonal unit cell. If a larger ion is put at that site a compensation of the extra volume in c-direction is complicated, but in a-direction it might be possible by twisting the neighbouring base planes of the tetrahedron against each other. From our unit cell data for CZP and SZP determined at room temperature we can estimate a twist angle of 1.4° around the c-direction, which indeed can shorten the lattice parameter a.

From Fig. 8 one can conclude that the thermal expansion coefficient of CSZP solid solutions is tailorable. CZP contracts along a-axis and expands along c-axis with rising

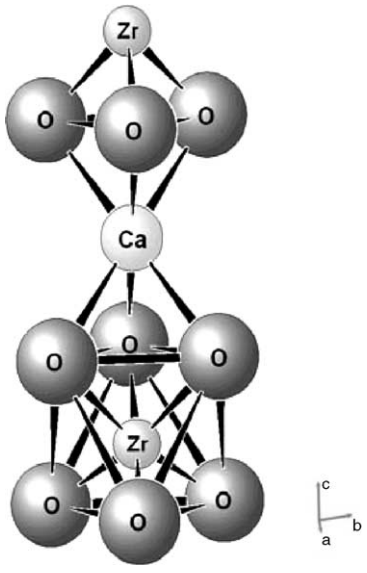

Fig. 9. Cut-out of the hexagonal unit cell of CSZP showing the Ca/Sr site between two oxygen triangles.

temperature, while SZP expands along both axes. By selecting an appropriate composition in this solid solution series it should be possible to minimize the thermal expansion.

The high-temperature X-ray data clearly indicate anisotropy in thermal expansion properties for most of the solid solutions, which match well with the reported values available in the literature (Table 7). In this study, SZP exhibits almost isotropic behaviour up to 1000 °C. However, its unit cell volume increases by about 0.8% which is by far the highest in the investigated compounds (Fig. 8) and challenges its utility. To the contrary, CZP records only a marginal increase in unit cell volume through out the temperature range, although in this case the ratio c/a increases by about 1.5%. This different behaviour of unit cell expansion and structural anisotropy needs further studies with respect to consequences for properties of bulk samples of this material. With respect

Table 7
Comparison of the thermal expansion data of the powder samples with the reported results

Sample	$\alpha_a/10^{-6}\,K^{-1}$			$\alpha_c/10^{-6}\,K^{-1}$		
	This study	Limaye et al.[13]	Kutty et. al.[22]	This study	Limaye et al.[13]	Kutty et. al.[22]
CZP	−3.3(1)	−5.1	−2.57	10.1(2)	9.9	7.74
CSZP(I)	−1.0(8)	–	–	8.4(1)	–	–
CSZP(II)	−0.2(1)	−0.7	–	5.8(2)	1.1	–
SZP	0.2(1)	3.6	2.24	3.3(1)	−1.2	2.28

to minimization of both parameters simultaneously the compound CSZP(II) should be preferred for engineering applications.

5. Summary

Several compounds of $Ca_{1-x}Sr_xZr_4(PO_4)_6$ ($0 \leq x \leq 1$) were synthesized by solid-state reaction route. The lattice parameters of the hexagonal unit cell were determined at room temperature and up to 1000 °C. The microscopic thermal expansion data showed different behaviour of this solid solution series with respect to anisotropy and volume expansion. The results pointed out that with increasing Sr content the thermal anisotropy decreases and the volume expansion increases which points to the existence of a composition with a minimal thermal expansion. The present investigation let conclude that within this series $Ca_{0.5}Sr_{0.5}Zr_4(PO_4)_6$ has this property which is desirable for different engineering applications.

The bulk thermal expansion coefficients of the material showed the same tendencies like the microscopic ones, although the absolute values were different from those of the corresponding powders. The powder samples were sintered up to 98% of the theoretical density adding 3 and 5 wt.% ZnO as sintering aid.

Acknowledgments

The authors are grateful to Aeronautic Research and Development Board of India for partially funding this activity. Part of this activity was carried out under the Indo-German collaborative programme on "Microstructural Characterisation of Thermal Barrier Coating by Indentation Method". The authors express their thanks to all participating members, especially to Dr. H.S. Maiti, (CGCRI Kolkata), for supporting in different manner the progress of this study.

References

1. Hong, H. Y. P., Crystal structures and crystal chemistry in the system $Na_{1+x}Zr_2Si_xP_{3-x}O_{12}$. *Mater. Res. Bull.*, 1976, **11**, 173.
2. Volkov, Ju. F. and Orlova, A. I., Formula type systematics of orthophosphates of one-, two-, three-, four- and five-valent elements. *Radiochemistry*, 1996, **38**, 15.
3. Goodenough, J. B., Hong, H. Y. P. and Kafalas, J. A., Fast Na^{2+} ion transport in skeleton structures. *Mater. Res. Bull.*, 1976, **11**, 203.
4. Alamo, J. and Roy, R., Ultra-low expansion ceramics in the system Na_2O–ZrO_2–P_2O_5–SiO_2. *J. Am. Ceram. Soc.*, 1984, **67**, 78.
5. Oota, T. and Yamai, I., Thermal expansion behaviour of $NaZr_2(PO_4)_3$-type compounds. *J. Am. Ceram. Soc.*, 1986, **69**, 1.
6. Agarwal, D. K., Harshe, G., Breval, E. and Roy, R. A., $NaZr_2P_3O_{12}$-type materials for protection of carbon-carbon composites. *J. Mater. Res.*, 1996, **11**, 3158.
7. Roy, R., Agarwal, D. K., Alamo, J. and Roy, R. A., [CTP]; A new structural family of near-zero expansion ceramics. *Mater. Res. Bull.*, 1984, **19**, 471.
8. Agarwal, D. K. and Stubican, V. S., Synthesis and sintering of $Ca_{0.5}Zr_2P_3O_{12}$—a low thermal expansion material. *Mater. Res. Bull.*, 1985, **20**, 99.
9. Roy, R., Agarwal, D. K. and Roy, R. A. US Patent 4675302, issued 23 June 1987.
10. Yoon, Ch. S., Kim, J. H., Kim, Ch. K. and Hong, K. S., Synthesis of low thermal expansion ceramics based on $CaZr_4(PO_4)_6$–LiO_2 system. *Mater. Sci. Eng.*, 2001, **B79**, 6.
11. Taylor, D., Thermal expansion data XIV, complex oxides with the sodalite and nasicon framework structures. *Br. Ceram. Trans.*, 1991, **90**, 64.
12. Breval, E. and Agrawal, D. K., Thermal expansion characteristics of [NZP], $NaZr_2P_3O_{12}$-type materials: a review. *Br. Ceram. Trans.*, 1995, **94**, 27.
13. Limaye, S. Y., Agarwal, D. K., Roy, R. and Mehrotra, Y., Synthesis, sintering, and thermal expansion of $Ca_{1-x}Sr_xZr_4P_6O_{24}$—an ultra-low thermal expansion ceramic system. *J. Mater. Sci.*, 1991, **26**, 93.
14. Limaye, S. Y., Agrawal, D. K. and Mckinstry, H. A., Synthesis and thermal expansion of $MZr_4P_6O_{24}$ (M = Mg, Ca, Sr, Ba). *J. Am. Ceram. Soc.*, 1987, **10**, C232.
15. Agrawal, D. K., NZP: a new family of low thermal expansion ceramics. *Trans. Ind. Ceram. Soc.*, 1996, **55**, 1.
16. Huang, C. Y., Agarwal, D. K. and McKinstry, H. A., Synthesis and thermal expansion behaviour of $Ba_{1+x}Zr_4P_{6-2x}Si_{2x}O_{24}$ and $Sr_{1+x}Zr_4P_{6-2x}Si_{2x}O_{24}$. *J. Mater. Res.*, 1994, **9**, 2005.
17. Fischer, W., Singheiser, L., Dasgupta, A. and Basu, D., Crystal structure of $Ca_{1-x}Sr_xZr_4(PO_4)_6$ ($0 \leq x \leq 1$). *Powder Diffraction*, 2004, **19**, 53.
18. Oota, T., Jin, P. and Yamai, I., Low thermal expansion and thermal expansion anisotropy ceramic system $Sr_{0.5}Zr_2(PO_4)_3$. *J. Mater. Sci.*, 1989, **24**, 4239.
19. Angadi, B., Jali, V. M., Lagare, M. T., Kini, N. S. and Umarji, A. M., Synthesis and thermal expansion hysteresis of $Ca_{1-x}Sr_xZr_4P_6O_{24}$. *Mater. Sci. Bull.*, 2002, **25**, 191.
20. Brochu, R., El-Yacoubi, M., Louer, M., Serghini, A. and Louer, D., Crystal chemistry and thermal expansion of $Cd_{0.5}Zr_2(PO_4)_3$ and $Cd_{0.25}Sr_{0.25}Zr_2(PO_4)_3$ ceramics. *Mater. Res. Bull.*, 1997, **32**, 15.
21. Lenain, G. E., McKinstry, H. A., Alamo, J. and Agarwal, D. K., Structural model for structural expansion in $MZr_2P_3O_{12}$ (M = Li, Na, K, Rb, Cs). *J. Mater. Sci.*, 1987, **22**, 17.
22. Govindan Kutty, K. V., Asuvathraman, R. and Sridharan, R., Thermal expansion studies on the sodium zirconium phosphate family of compounds $A_{1/2}M_2(PO_4)_3$: effect of interstitial and framework cations. *J. Mater. Sci.*, 1998, **33**, 4007.
23. Agarwal, D. K., Huang, C. Y. and McKinstry, H. A., NZP: a new family of low-thermal expansion materials. *Int. J. Theor. Phys.*, 1991, **12**, 697.